有机化学 DOI: 10.6023/cjoc202305006 研究论文
Chinese Journal of Organic Chemistry ARTICLE

硅烷桥联四苯乙烯-寡聚噻吩衍生物的结构与光谱性质

余富欢 周志宽* 谢 威 周传庭 盖立志 卢 华*
(杭州师范大学材料与化学化工学院 有机硅化学及材料技术教育部重点实验室 杭州 311121)

摘要 设计合成了一系列硅烷桥联四苯乙烯(TPE)-寡聚噻吩衍生物. 硅烷取代基为甲基和苯基, 寡聚噻吩单元中噻吩数量为 1～3, 通过空间位阻效应和电子效应调控分子的固态发光性质. 具有苯基取代基的硅烷和二噻吩分子表现出高达 64.5%的固态发光. 含 1 或 2 个噻吩单元的分子的固态和液态荧光性质类似四苯乙烯, 而含 3 个噻吩的分子的发光则主要来自于三噻吩, 其在液态和聚集态分别有 1.4%和 14%的发光效率. 苯基硅烷桥联三噻吩-四苯乙烯分子的聚集体具有检测硝基爆炸物的能力和防伪应用潜力.

关键词 硅烷; 四苯乙烯; 寡聚硅烷; 荧光

Structure and Photophysical Properties of Silane Bridged Tetraphenylethylene-Oligothiophene Derivatives

Yu, Fuhuan Zhou, Zhikuan* Xie, Wei Zhou, Chuanting Gai, Lizhi Lu, Hua*
(*Key Laboratory of Organosilicon Chemistry and Material Technology*, *Ministry of Education*, *College of Material Chemistry and Chemical Engineering*, *Hangzhou Normal University*, *Hangzhou 311121*)

Abstract A series of silane-bridged tetraphenylethene (TPE)-oligothiophene derivatives were synthesized. The silane substituents varied from methyl to phenyl groups, while the number of thiophene units in the oligothiophene segment was 1 to 3. The solid-state luminescence properties of the molecules were regulated by steric hindrance and electronic effects. Phenyl substituted silane-bridged bithiophene (BT)-TPE molecules exhibited up to 64.5% solid-state luminescence. Molecules containing 1 or 2 thiophene units exhibited fluorescence properties similar to TPE in both solid and liquid states, while the emission of molecules containing 3 thiophene units mainly came from terthiophene (TT) with luminescence efficiencies of 1.4% and 14% in liquid and aggregated states, respectively. The aggregate of phenyl substituted silane-bridged TT-TPE molecules exhibited potential for detecting nitro explosives and anti-counterfeiting applications.

Keywords silane; tetraphenylethene; oligothiophene; luminescence

1 Introduction

Organosilicon compounds are widely used in organic synthesis and material science.[1-9] In organic optoelectronic molecules, the bridging silicon units can effectively interrupt molecular conjugation which result in full separation of the highest occupied molecular orbital (HOMO)-lowest unoccupied molecular orbital (LUMO) energy levels and increased triplet energy levels.[10] As a result, they have become ideal hosts materials.[11] Tetraphenylsilane is commonly employed to increase intermolecular steric hindrance to manipulate solid-state emission[12] and exciton-utilizing efficiencies.[13] When incorporated into carbon based aromatic cycles, silicon can interact with π systems through σ*-π* conjugation, these silicon-containing compounds usually exhibit rigid structures and redshifted absorption and emission.[14-18] Therefore, organosilicon has significant advantages in regulating the structure and properties of functional molecules.

Oligothiophenes are important electron transport and light harvest building blocks employed in optoelectronic and optical materials.[19] Introduction of silyl substituents[20-21] and construction of donor (D)-Si-acceptor (A) type architectures[22-24] have demonstrated to be efficient ways to modulate the luminescent properties of oligothiophenes. However, even with these carefully designed oligothiophene derivatives, their solid-state fluorescence efficiencies remain very low, mostly below 1%. This greatly

* Corresponding authors. E-mail: zkzhou@hznu.du.cn; hualu@hznu.edu.cn
Received May 7, 2023; revised May 26, 2023; published online June 13, 2023.
Project supported by the National Natural Science Foundation of China (Nos. 21871072, 21801057) and the Hangzhou Leading Youth Innovation and Entrepreneurship Team Project (No. TD2020015).
国家自然科学基金(Nos. 21871072, 21801057)和杭州市领军型创新创业团队(No. TD2020015)资助项目.

limits the practical application of oligothiophenes in luminescent materials.

A simple way to enhance the solid-state luminescence of oligothiophenes is to attach aggregation-induced emission (AIE) luminogens such as tetraphenylethene (TPE)[25-27] to the thiophene unit.[28] However, the attachment of TPE to classic organic fluorophores usually results in aggregation-caused quenching (ACQ) effect in solution.[29] Only a few TPE-based dual-state emitters based on self-assembly system were reported.[30-32] Based on our previous research in the field of organosilicon luminescent materials,[12-13,15,33-37] we speculate that the introduction of substituted silane bridges between TPE and oligothiophene may enhance the luminescence properties of oligothiophene in both solid and liquid states. In this work, we designed a silane-bridged TPE-oligothiophene derivatives. The silane substituents varied from methyl to phenyl groups, oligothiophene such as thiophene, bithiophene (BT), and terthiophene (TT) were employed. The structures, photophysical properties, as well as their application in explosive detection and anti-counterfeiting were examined.

2 Results and discussion

2.1 Synthesis

The synthetic routes to target compounds **3**～**6b** are shown in Scheme 1. Brominated TPE **1** was subjected to lithium-halogen exchange reaction to obtain TPE lithiation reagent, which reacted *in situ* with 1 equiv. of dichlorodimethylsilane or dichlorodiphenylsilane, followed by reduction with $LiAlH_4$ to obtain tertiary silane compound **2**.[33] It underwent a Rh-catalyzed Si—C coupling reaction[38] with a series of aryl diiodide compound to yield the target compounds **3**～**6b**. The chemical structures of all the compounds were verified by ^1H NMR, ^{13}C NMR and HRMS-ESI.

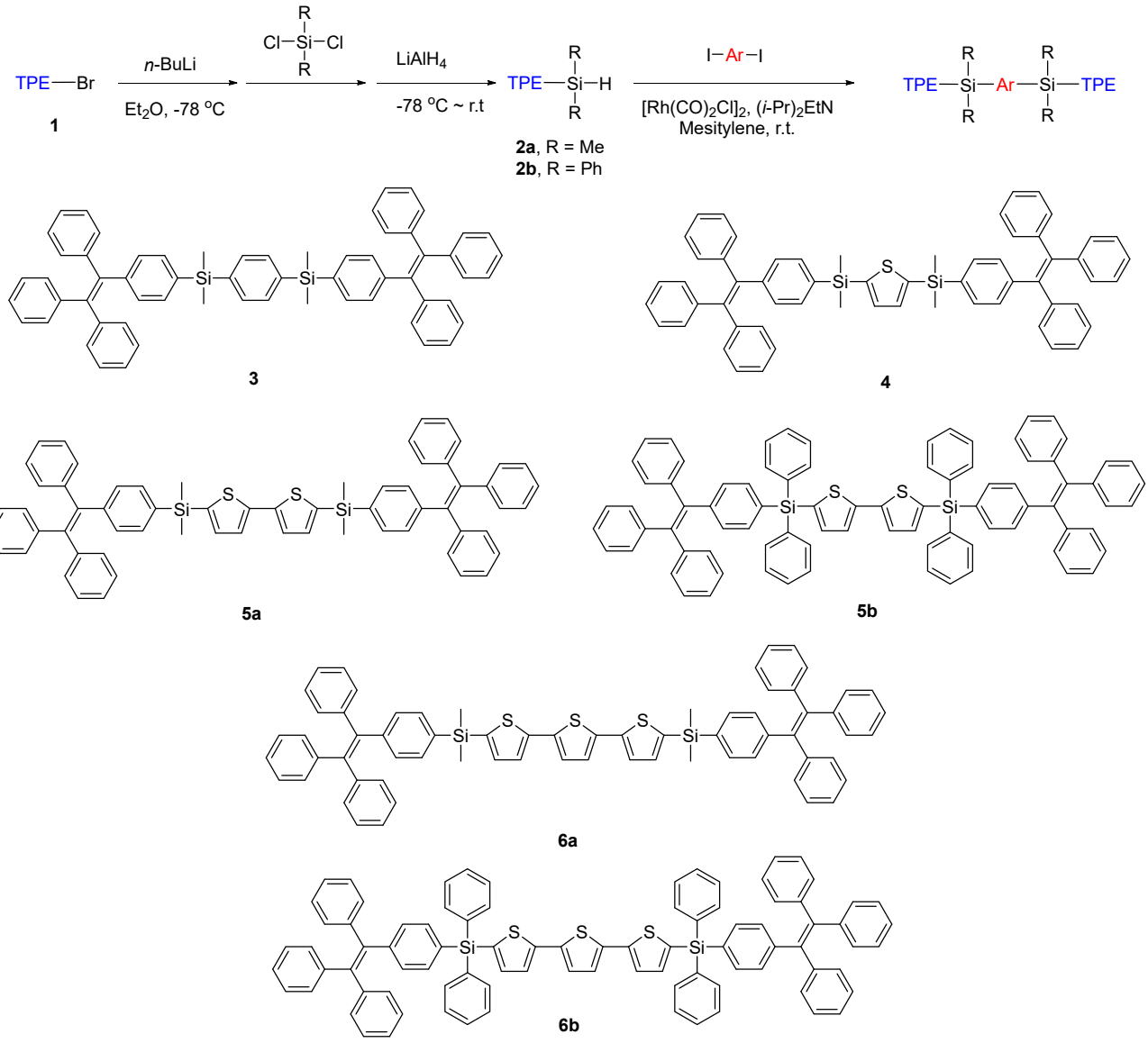

Scheme 1 Synthetic routes and chemical structures of **3**～**6b**

2.2 UV absorption in tetrahydrofuran (THF) solution

The UV absorption spectra of compounds **3**～**6b** in THF solution is shown in Figure 1. For comparison, the absorption spectra of monomers TPE, BT and TT are also shown. The absorption spectra of **3** and **4** almost overlap with the same maxima located at 313 nm, which can be attributed to the π-π* transition of the TPE unit.[39-40] No contributions from the central benzene and thiophene units are observed, since their absorption maxima locate at 240 and 260 nm, respectively.[41] The absorption maxima of **5a** and **5b** slightly redshift to 320 and 323 nm. Compounds **6a** and **6b** show UV spectra that are very different from those of **3**～**5**. Broad dual absorption peaks are observed at 326 and 363 nm for **6a**, and 326 and 370 nm for **6b**. The high energy UV absorption peaks at 326 nm originate from TPE (λ_{max}＝306 nm), while the low energy peaks at 363～370 nm may be attributed to TT (λ_{max}＝356 nm). It is noteworthy that the absorption profiles of compounds **3**～**6** appear to be a superposition of their building blocks TPE, BT and TT, which show the absorption maxima peaking at 304, 310 and 356 nm, respectively. The observed 10～20 nm redshift of absorption peaks of dyads compared with the monomers indicate the existence of intramolecular charge transfer.

2.3 Fluorescence in solution and aggregated state

As presented in Figure 2 and Table 1, the fluorescences of compounds **3**～**5** in THF are very weak with quite low

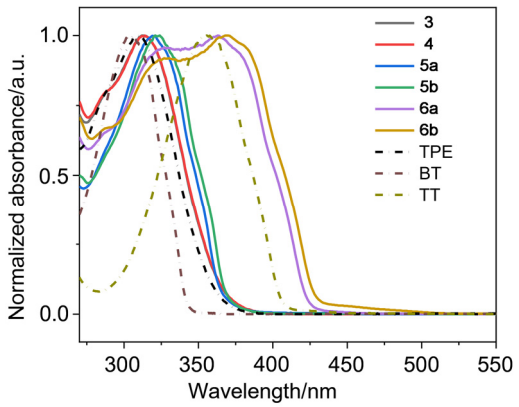

Figure 1 UV absorption spectra of compounds **3**～**6**, TPE, BT, and TT in THF.

fluorescence efficiency (Φ_F 0.4%～0.5%). Compounds **6a** and **6b** exhibit dual peak emission with relatively higher fluorescence efficiency (Φ_F＝1.4%). However, these compounds show drastically increased fluorescence with Φ_F ranging from 10.3% to 64.5% in powder forms, which are 7 to 129-fold of that in solution. The solid-state fluorescence quantum yields of BT and TT reported in the literature are only 0.01 and 0.08, respectively.[21] The emission color of compounds **3**～**6** changes from blue to sky blue, and then to green and finally yellow. The full width at half maximum (FWHM) is between 95 and 114 nm, which

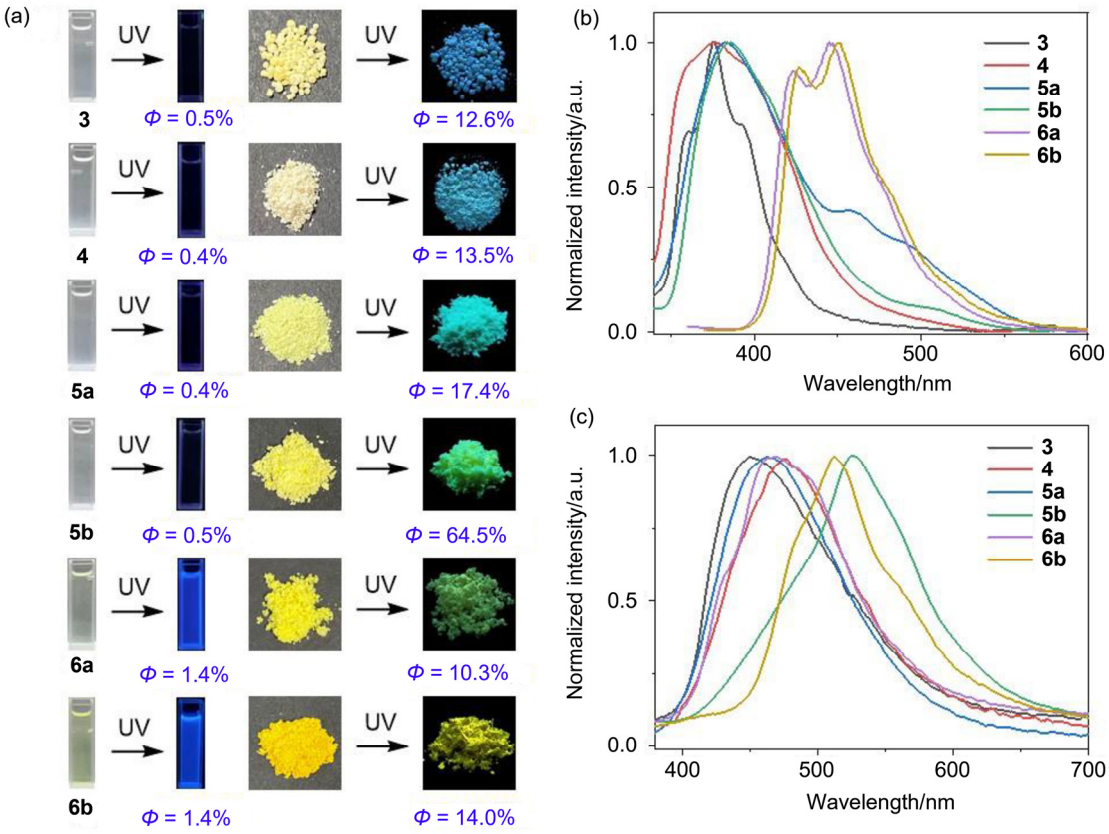

Figure 2 (a) Photographs of compounds **3**～**6** before and after UV irradiation in THF solution and powder form, and fluorescence spectra of compounds **3**～**6** in (b) THF solution and (c) solid powders

is larger than that of TPE. The maximum emission wavelength of compound **3** is 450 nm, which is the same with TPE.[34] The maximum emission wavelengths of compounds **4**, **5a** and **6a** are 475, 463 and 467 nm, respectively, which exhibit 13～25 nm redshift compared with TPE. Interestingly, the maximum emission wavelengths of **5b** and **6b** are 526 and 512 nm, respectively, and their fluorescent quantum yields are higher than **5a** and **6a**, which indicates that the phenyl groups on silicon facilitating regular packing of molecules in the solid state. These results demonstrate that the type of central oligothiophene unit determines the emission of dyads in solution, while in the solid state the substituent on silicon atoms is the key factor affecting the emission properties of dyads.

The fluorescence quantum yields of these compounds in their powder state are 7～129 times higher than that in solution, indicating their aggregation-induced emission (AIE) activities. The changes in fluorescence intensity of these compounds in THF/water mixture with various fractions (f_w) are shown on Figure 3. Compounds **3**, **4**, **5a** and **5b** exhibit similar AIE properties. The solutions do not emit significant fluorescence when f_w is less than or equal to 60%. However, the fluorescence intensity increases significantly when f_w exceeds 70%. The fluorescence intensity reaches its maximum value when f_w reaches 95%.

Interestingly, **6a** and **6b** exhibit two sets of fluorescence emission peaks in THF/water mixtures. In pure THF, the dual emission peaks at the short wavelength arise from the fluorescence of TT unit, which are located at 422 and 445 nm for **6a** and 426 and 450 nm for **6b**, respectively. As f_w

Table 1 Absorption and fluorescence data of compounds **3**～**6b** in THF, 95% H_2O/THF, and powder forms.

Compd.	λ_{abs}/nm	THF		95% H_2O/THF		Powder	
		λ_{em}/nm	QY[a]/%	λ_{em}/nm	QY[a]/%	λ_{em}/nm	QY[a]/%
3	313	376	0.5	468	26.7	450	12.6
4	313	376	0.4	471	21.2	475	13.5
5a	320	383	0.4	469	21.2	463	17.4
5b	323	385	0.5	469	31.6	526	64.5
6a	326, 363	423, 446	1.4	465, 495	7.2	467	10.3
6b	326, 370	427, 450	1.4	521, 556	23.9	512	14.0

[a] Absolute quantum yields measured in powder with an integration sphere.

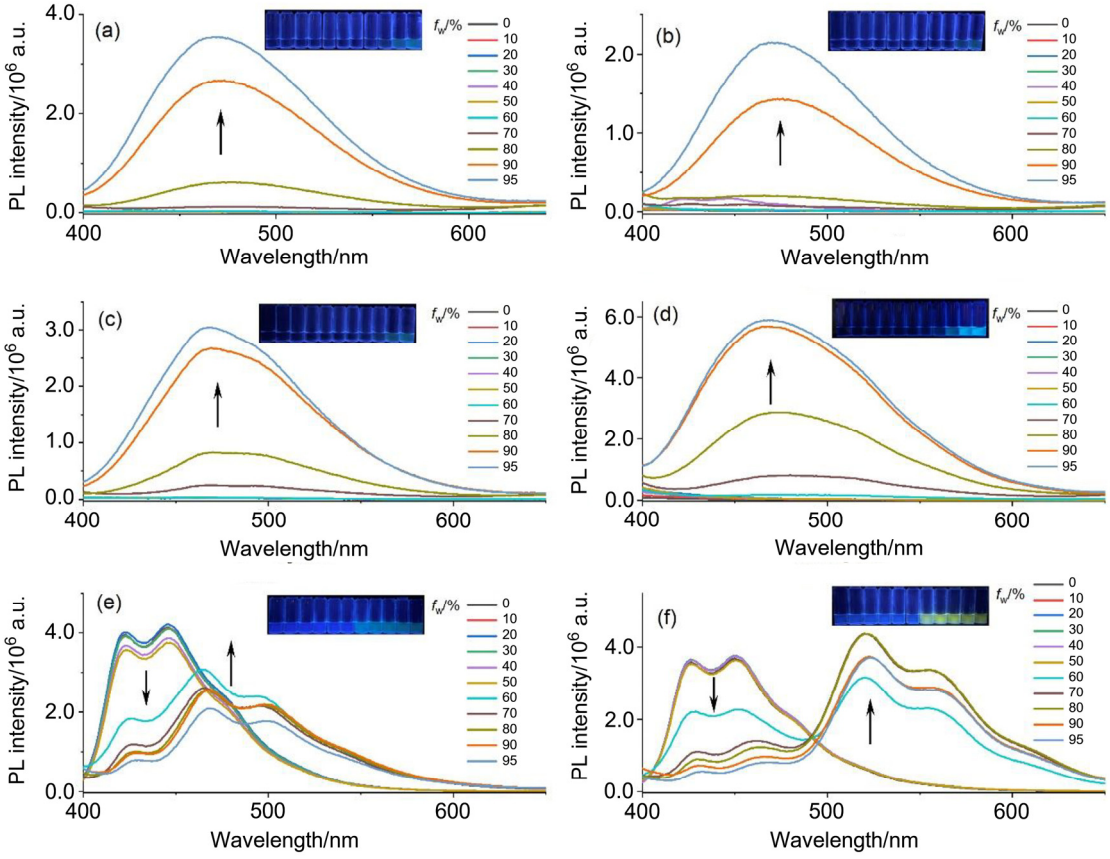

Figure 3 Emission spectra of compounds (a) **3**, (b) **4**, (c) **5a**, (d) **5b**, (e) **6a** and (f) **6b** in various THF/water mixtures
Inserts show the photographs of compounds in mixed solvents under 365 nm UV irradiation. f_w: the proportion of water in the total solvent volume ($f_w = V_{water}/(V_{THF}+V_{water})$, where V is volume.

reaches 60%, the intensity of these emission peaks suddenly decreases. At the same time, a new set of AIE peaks raise up, which are located at 465 and 497 nm for **6a**, and 520 and 556 nm for **6b**. As the water fraction increases, the emission color of compound **6a** changes from blue to sky blue, while that of compound **6b** changes from blue to yellow. In the pure solution state, the TPE units in the molecule do not quench the fluorescence of these two compounds, and even at higher concentrations, their fluorescence intensity do not decrease. In the aggregated state, the solution luminescence disappears, and the luminescence of the molecular aggregates appears. From the emission wavelength point of view, the luminescence of the aggregates does not solely arise from TPE, but from the dye molecules as a whole.

2.4 Crystallographic analysis

Single crystals of **5a** and **6a** suitable for X-ray diffraction analysis (Figure 4) were obtained through gas-liquid two-phase diffusion of *n*-hexane into their dichloromethane solutions. **5a** belongs to the monoclinic crystal system. It exhibits a *Z*-shaped configuration, where two molecules interact with each other to form a unit in the crystal packing structure. The distance between two units is relatively large, and the overall stacking of molecules is loose. **6a** belongs to the triclinic crystal system. Two TPE units are embedded like earrings at the end of the two TT units. In the crystal packing structure, one TPE unit of a molecule interacts with one TPE unit of another molecule, forming a interlocking structure. The overall stacking of the molecules is also relatively loose. The relatively loose molecular stacking makes it easier for the phenyl rings within the molecule to rotate, resulting in exited states energy loss through non-radiative decay in the solid state and leading to lower luminescence efficiency.

2.5 Theoretical investigation

The quantum calculations of the frontier orbitals and excited states provide a better explanation for their optical properties. Density functional theory (DFT) and time-dependent DFT (TD-DFT) with B3LYP function and 6-31G(d) basis set were employed during the calculation. The HOMO energy levels of **3**, **4**, **5a**, and **5b** are almost the same with the electron density mainly located on TPE cores. The LUMOs of **3** and **4** are located on both TPE cores, while that of **5a** is located on BT core, and that of **5b** is located mainly on BT core and partially on vinyl group of TPE units. The HOMOs and LUMOs of **6a** and **6b** are localized on TT cores. The decrease of LUMO energy levels is the main reason for the decreasing HOMO-LUMO gaps (Figure 5). The TD-DFT calculation demonstrated that both the lowest energy absorption bands of **3** and **4** represented the HOMO−1→LUMO+1 transitions, which were assigned to π-π* absorption of TPE units. The lowest energy absorption band of **5a** was HOMO−2→LUMO transition, which was assigned to a π-π* excitation of BT units. The lowest energy absorption bands of **6a** and **6b** were the same HOMO→LUMO transition, which were assigned to π-π* excitation of TT units. Thus, the fluorescences of all these compounds were assigned to only π-π* emission from different units, and no ICT emission exists in such molecular systems.[42]

2.6 Application in explosive detection and anti-counterfeiting

The fluorescence titration spectra of compound **6b** with the addition of various explosives are shown in Figure 6.[43] As the control of explosives is highly regulated, only two common nitrobenzene compounds were obtained for testing purposes. Significant reductions in fluorescence are observed in mixtures with f_w=95% as the concentration of guest molecules, such as nitrobenzene and 4-nitrotoluene, increases. Unlike a previous report on organic solvents, the quenching response still operates in aqueous media at f_w=95%. The quenching percentage of fluorescence intensity is 13% in the presence of 2.25 equiv. of nitrobenzene, while the quenching percentage is 27% for 4-nitrotoluene in the same condition.

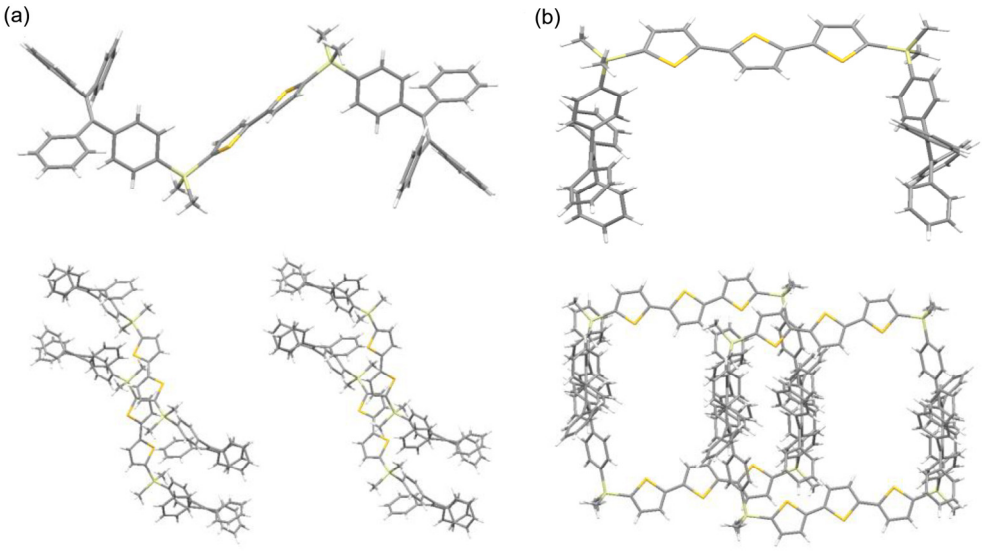

Figure 4 Single crystal structures and crystal packings of (a) **5a** (CCDC 2252772) and (b) **6a** (CCDC 2252773)

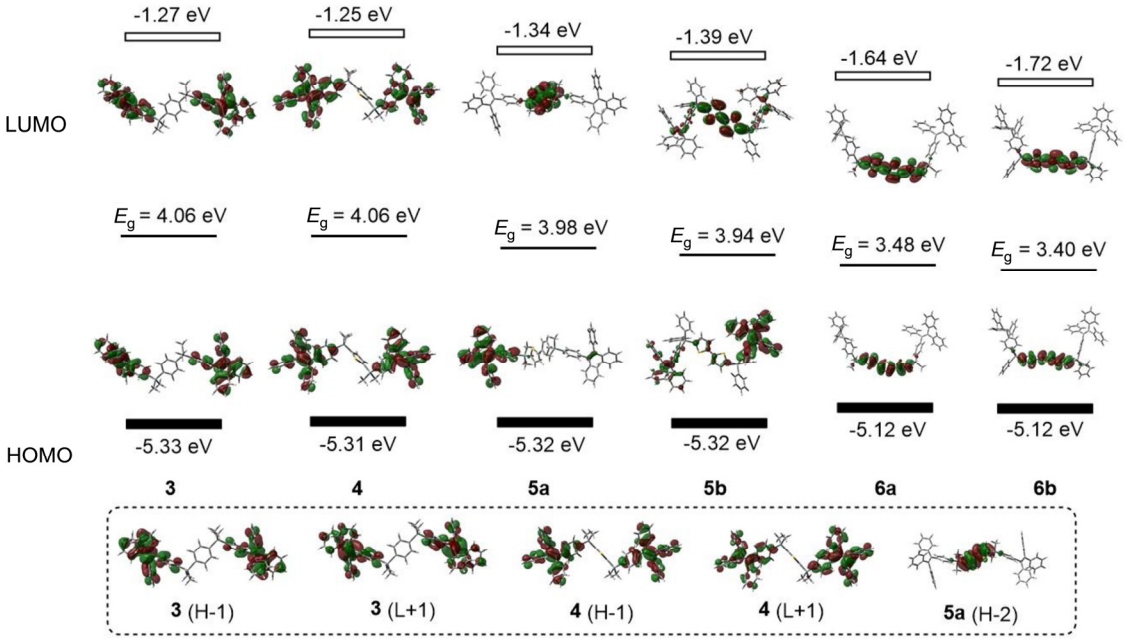

Figure 5 HOMOs and LUMOs of **3**～**6b** calculated with B3LYP/6-31G(d) level

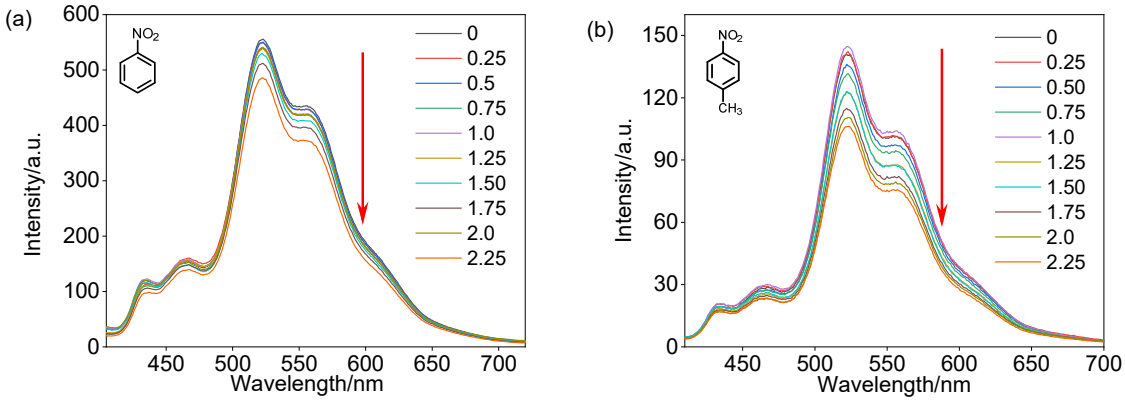

Figure 6 Fluorescence titration spectra of compound **6b** with various equivalents of (a) nitrobenzene and (b) 4-nitrotoluene in THF/water mixtures where f_w=95%

The anti-counterfeiting properties of compound **6b** was tested. The inks containing TPE and **6b** were used to write "HZNU" on filter paper, respectively (Figure 7). The characters appeared almost colorless under sunlight. Under 365 nm UV light, the characters written with TPE ink emitted blue color, while those written with **6b** ink appeared yellow-green. After completely immersing the filter paper in ethanol, the text written with **6b** ink still emitted bright yellow-green light, while the text written with TPE ink became blurry. After air-drying the filter paper, the text written with **6b** ink remained clearly visible. These experiments demonstrate that **6b** has strong adhesion on paper and is not dissolved by disinfectant alcohol or even ethanol. This can extend its application scenarios in real life.

3 Conclusions

In summary, through the study of the structures and photophysical properties of silane-bridged TPE-oligothiophene derivatives, it was found that phenyl-substituted silane as a bridge can enhance the solid-state luminescence, and compound **5b** exhibits the highest solid-state fluorescence quantum yield of 64.5%. For small aromatic units such as benzene, thiophene, and bithiophene, the silane-bridged TPE derivatives exhibit classical AIE properties similar to TPE. On the other hand, TPE-Si-terthiophene derivatives exhibit dual-state emission with quantum yields of 1.4% and 14.0% in solution and solid states, respectively. Aggregates of compound **6b** exhibit 27% fluorescence quenching in the presence of 4-nitrotoluene in aqueous solution. In addition, **6b** can be used as a fluorescent ink for paper anti-counterfeiting, and it can maintain good anti-counterfeiting performance in the presence of disinfectant alcohol or ethanol.

4 Experimental section

4.1 General methods

Reagents and solvents were purchased from commercial suppliers and used without further purification unless oth-

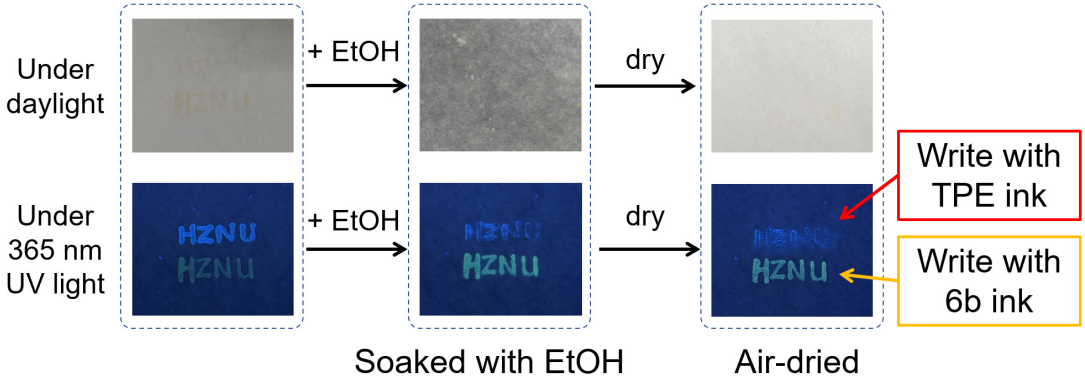

Figure 7 Fluorescence photographs of the letters "HZNU" written on filter papers using ink containing TPE (top line) and **6b** (bottom line) under different conditions

erwise indicated. All air and moisture-sensitive reactions were carried out under an argon atmosphere in glassware that was dried in an oven at 120 ℃ and cooled under a stream of inert gas before use. Tetrahydrofuran was refluxed with sodium and distilled out immediately before use. ^{1}H NMR and ^{13}C NMR spectra were recorded on a Bruker DRX400 spectrometer and referenced to the residual proton signals of deuterated solvents ($CDCl_3$ δ 7.26). HRMS data were recorded on a Bruker Daltonics micro-TOF-Q II spectrometer. All solvents used for the spectroscopic measurements were of UV spectroscopic grade (Aldrich).

4.2 Synthesis

4.2.1 Synthesis of diphenyl(4-(1,2,2-triphenylvinyl)-phenyl)silane (**2b**)

In a 100 mL Schlenk tube, (2-(4-bromophenyl)ethene-1,1,2-triyl)tribenzene (TPE-Br, **1**) (2 g, 5 mmol) was dissolved in dry ether under argon and cooled to −78 ℃, then *n*-BuLi (3.2 mL, 5 mmol, 1.6 mol/L in *n*-hexane) was added dropwise. The mixture was stirred at −78 ℃ for 1 h and then warmed to 0 ℃. In another 100 mL Schlenk tube, dichlorodiphenylsilane (1.05 mL, 5 mmol) was dissolved in dry ether (50 mL) under argon and cooled to −78 ℃. The previous TPE-Li mixture was transferred into the flask and stirred for 2 h. The reaction mixture was gradually warmed up to room temperature, then $LiAlH_4$ (190 mg, 5.0 mmol) was added, and the mixture was stirred overnight. The reaction was carefully quenched with water (3 mL), then 10 mL of THF was added and the mixture was filtered to remove insoluble materials. The organic layer was dried over sodium sulfate. The solvent was evaporated under vacuo and the residues were purified by chromatography over silica gel (dichloromethane/petroleum ether, V∶V=1∶9) to give compound **2b** as a white powder (1.54 g, 60%). m.p. 152～154 ℃; ^{1}H NMR (400 MHz, $CDCl_3$) δ: 7.53 (dd, J=7.8, 1.7 Hz, 4H), 7.43～7.32 (m, 8H), 7.14～7.09 (m, 10H), 7.05 (d, J=8.8 Hz, 9H), 5.42 (s, 1H); ^{13}C NMR (100 MHz, $CDCl_3$) δ: 145.4, 143.7, 143.5, 141.6, 140.9, 135.9, 135.3, 133.6, 131.5, 131.5, 131.0, 129.9, 128.1, 127.8, 127.8, 127.7, 126.7, 126.6.

4.2.2 Synthesis of compounds **3**～**6**

Dimethyl(4-(1,2,2-triphenylvinyl)phenyl)silane (TPE-dimethylsilane, **2a**) (390 mg, 1.0 mmol), 1,4-diiodobenzene (165 mg, 0.5 mmol) and rhodium carbonyl chloride (8 mg, 0.015 mmol) were added into a 10 mL Schlenk tube under argon. Dry mesitylene (3 mL) was added and the reaction mixture was stirred at room temperature for 10 min. *N*,*N*-Diisopropylethylamine (0.13 mL, 0.75 mmol) was added dropwise. The reaction was carried out at room temperature for 3 d. When the reactants have been fully consumed detected by thin-layer chromatography (TLC), the reaction was stopped and the insoluble material was removed by filtration. The solvent was evaporated under reduced pressure in vacuo, and the resulting crude product was purified by column chromatography with 200～300 mesh silica gel (eluent: dichloromethane/petroleum ether, V∶V=1∶10), and then recrystallized from *n*-pentane to obtain a light yellow solid powder as compound **3** (166 mg, 9.7%). **4**, **5a**, **5b**, **6a** and **6b** were obtained by using the same procedure as compound **3** with TPE-diphenylsilane, 5,5'-diiodo-2,2'-bithiophene and 5,5''-diiodo-2,2':5',2''-terthiophene as starting materials.

1,4-Bis(dimethyl(4-(1,2,2-triphenylvinyl)phenyl)silyl)-benzene (**3**): m.p. 173～175 ℃; ^{1}H NMR (400 MHz, $CDCl_3$) δ: 7.12 (s, 1H), 7.10 (s, 3H), 6.98～6.83 (m, 38H), 0.34 (s, 12H); ^{13}C NMR (100 MHz, $CDCl_3$) δ: 144.57, 143.87, 143.78, 141.28, 141.04, 139.44, 135.80, 133.65, 133.51, 131.48, 130.74, 127.78, 126.54; HRMS (ESI$^+$) calcd for $C_{62}H_{54}Si_2$ 854.3764, found 854.3745.

2,5-Bis(dimethyl(4-(1,2,2-triphenylvinyl)phenyl)silyl)-thiophene (**4**): 5.7% yield, light yellow solid powder. m.p. 74～75 ℃; ^{1}H NMR (400 MHz, $CDCl_3$) δ: 7.30 (d, J=8.0 Hz, 2H), 7.19 (d, J=8.0 Hz, 2H), 7.14～6.95 (m, 36H), 0.54 (s, 7H), 0.21 (s, 5H); ^{13}C NMR (100 MHz, $CDCl_3$) δ 137.3, 136.3, 135.9, 134.9, 134.6, 131.4, 131.0, 129.9, 128.1, 127.8, 126.6, 107.8, 106.5, 29.6, 24.0; HRMS (ESI$^+$) calcd for $C_{60}H_{52}SSi_2$ 860.3328, found 860.3342.

5,5'-Bis(dimethyl(4-(1,2,2-triphenylvinyl)phenyl)silyl)-2,2'-bithiophene (**5a**): 10.4% yield, yellow solid powder. m.p. 101～103 ℃; ^{1}H NMR (400 MHz, $CDCl_3$) δ: 7.31 (d, J=7.7 Hz, 4H), 7.22 (d, J=3.4 Hz, 2H), 7.14～7.01 (m,

38H), 0.55 (s, 12H); ^{13}C NMR (100 MHz, $CDCl_3$) δ: 146.2, 145.1, 145.0, 144.4, 142.7, 142.2, 139.4, 137.4, 136.5, 134.6, 132.7, 132.1, 129.0, 129.0, 127.9, 127.8, 126.4; HRMS (ESI$^+$) calcd for $C_{64}H_{54}S_2Si_2$ 942.3205, found 942.3215.

5,5'-Bis(diphenyl(4-(1,2,2-triphenylvinyl)phenyl)silyl)-2,2'-bithiophene **5b**: 25.6% yield, yellow solid powder. m.p. 137～139 ℃; ^{1}H NMR (400 MHz, $CDCl_3$) δ: 7.57 (d, J=7.1 Hz, 8H), 7.41 (td, J=17.4, 16.5, 7.7 Hz, 16H), 7.30 (s, 2H), 7.10 (d, J=12.3 Hz, 36H); ^{13}C NMR (100 MHz, $CDCl_3$) δ: 145.7, 144.4, 143.7, 143.6, 143.4, 141.7, 141.0, 139.2, 136.2, 135.5, 134.0, 133.9, 131.5, 131.5, 130.9, 130.0, 128.0, 127.8, 127.8, 127.7, 127.6, 126.6, 125.4; HRMS (ESI$^+$) calcd for $C_{84}H_{62}S_2Si_2$ 1190.3831, found 1190.3855.

5,5''-Bis(dimethyl(4-(1,2,2-triphenylvinyl)phenyl)silyl)-2,2':5',2''-terthiophene (**6a**): 15.0% yield, yellow solid powder. m.p. 86～87 ℃; ^{1}H NMR (400 MHz, $CDCl_3$) δ: 7.32 (d, J=7.7 Hz, 4H), 7.21 (d, J=3.5 Hz, 2H), 7.06 (dd, J=22.0, 6.2 Hz, 38H), 0.55 (s, 12H); ^{13}C NMR (100 MHz, $CDCl_3$) δ: 145.0, 143.8, 143.7, 142.9, 141.4, 140.9, 138.2, 136.4, 136.2, 135.1, 133.4, 131.5, 130.9, 127.8, 126.6, 125.0, 124.6; HRMS (ESI$^+$) calcd for $C_{68}H_{56}S_3Si_2$ 1024.3083, found 1024.3091.

5,5''-Bis(diphenyl(4-(1,2,2-triphenylvinyl)phenyl)silyl)-2,2':5',2''-terthiophene (**6b**): 5.8% yield, yellow solid powder. m.p. 268～270 ℃; ^{1}H NMR (400 MHz, $CDCl_3$) δ: 7.56 (s, 8H), 7.42 (d, J=19.0 Hz, 17H), 7.09 (d, J=15.6 Hz, 39H); ^{13}C NMR (100 MHz, $CDCl_3$) δ: 145.7, 144.3, 143.7, 143.6, 143.4, 141.7, 139.3, 136.2, 135.6, 133.9, 131.5, 131.5, 130.1, 128.1, 127.8, 127.7, 126.7, 126.6, 125.0, 124.9. HRMS (ESI$^+$) calcd for $C_{88}H_{64}S_3Si_2$ 1272.3709, found 1272.3731.

Supporting Information TD-DFT calculated UV absorption, ^{1}NMR, and ^{13}C NMR spectra of compounds **3**～**6**. The Supporting Information is available free of charge via the Internet at http://sioc-journal.cn.

References

[1] Wang, H.; Zhang, X.; Li, Y. Xu, L.-W. *Angew. Chem., Int. Ed.* **2022**, *61*, e202210851.

[2] Ding, Y.; Zhang, J.; Li, Y.; Cui, C. *J. Am. Chem. Soc.* **2022**, *144*, 20566.

[3] Zuo, Y.; Liang, X.; Yin, J.; Gou, Z.; Lin, W. *Coord. Chem. Rev.* **2021**, *447*, 214166.

[4] Wang, H.; Chen, S.; Li, Y.; Liu, Y.; Jing, Q.; Liu, X.; Liu, Z.; Zhang, X. *Adv. Energy Mater.* **2021**, *11*, 2101057.

[5] Shi, H.; Yang, J.; Li, Z.; He, C. In *Silicon Containing Hybrid Copolymers*, Wiley-VCH, Germany, **2020**, p. 1.

[6] Wang, X.-L.; Yin, X.-H.; Xiao, J.-Z.; Jia, X.-S.; Yin, L. *Chin. J. Chem.* **2021**, *39*, 1916.

[7] Yang, C.-H.; Chen, J. C.; Li, X.-H.; Meng, Li.; Wang, K.-M.; Sun, W.-Q.; Fan, B.-M. *Acta Chim. Sinica* **2023**, *81*, 1 (in Chinese).
(杨春晖, 陈景超, 李新汉, 孟丽, 王凯民, 孙蔚青, 樊保敏, 化学学报, **2023**, *81*, 1.)

[8] Huang, W.-S.; Xu, L.-W. *Chin. J. Org. Chem.* **2021**, *41*, 4515 (in Chinese).
(黄伟升, 徐利文, 有机化学, **2021**, *41*, 4515.)

[9] Cheng, Y.; Hu, R. J.; Chen, X.-Q.; Yang, H.; Niu, X.-K.; Yang, L. *Chin. J. Org. Chem.* **2022**, *42*, 323 (in Chinese).
(程异, 胡荣静, 陈晓琪, 杨浩, 牛晓康, 杨磊, 有机化学, **2022**, *42*, 323.)

[10] Liu, D.; Du, M.; Chen, D.; Ye, K.; Zhang, Z.; Liu, Y.; Wang, Y. *J. Mater. Chem. C* **2015**, *3*, 4394.

[11] Gong, S.; Chen, Y.; Luo, J.; Yang, C.; Zhong, C.; Qin, J.; Ma, D. *Adv. Funct. Mater.* **2011**, *21*, 1168.

[12] Lu, H.; Wang, Q.; Gai, L.; Li, Z.; Deng, Y.; Xiao, X.; Lai, G.; Shen, Z. *Chem.-Eur. J.* **2012**, *18*, 7852.

[13] Zheng, Y.; Wang, Z.; Wang, X.; Li, J.; Feng, X. J.; He, G.; Zhao, Z.; Lu, H. *ACS Appl. Electron. Mater.* **2021**, *3*, 422.

[14] Murai, M.; Abe, M.; Ogi, S.; Yamaguchi, S. *J. Am. Chem. Soc.* **2022**, *144*, 20385.

[15] Feng, S.; Qu, Z.; Zhou, Z.; Chen, J.; Gai, L.; Lu, H. *Chem. Commun.* **2021**, *57*, 11689.

[16] Tang, W.; Gao, H.; Li, J.; Wang, X.; Zhou, Z.; Gai, L.; Feng, X. J.; Tian, J.; Lu, H.; Guo, Z. *Chem.-Asian J.* **2020**, *15*, 2724.

[17] Tang, R.-H.; Xu, Z.; Nie, Y.-X.; Xiao, X.-Q.; Yang, K.-F.; Xie, J.-L.; Guo, B.; Yin, G.-W.; Yang, X.-M.; Xu, L.-W. *iScience* **2020**, *23*, 101268.

[18] Luo, Q.; Wang, W.; Tan, J.; Yuan, Q. *Chin. J. Chem.* **2021**, *39*, 1009.

[19] Zheng, Y.; Zhu, X.; Ni, Z.; Wang, X.; Zhong, Z.; Feng, X. J.; Zhao, Z.; Lu, H. *Adv. Opt. Mater.* **2021**, *9*, 2100965.

[20] Hirata, S.; Nishio, M.; Uchida, H.; Usuki, T.; Nakae, T.; Miyachi, M.; Yamanoi, Y.; Nishihara, H. *J. Phys. Chem. C* **2020**, *124*, 3277.

[21] Inubushi, H.; Hattori, Y.; Yamanoi, Y.; Nishihara, H. *J. Org. Chem.* **2014**, *79*, 2974.

[22] Sosorev, A. Y.; Nuraliev, M. K.; Feldman, E. V.; Maslennikov, D. R.; Borshchev, O. V.; Skorotetcky, M. S.; Surin, N. M.; Kazantsev, M. S.; Ponomarenko, S. A.; Paraschuk, D. Y. *Phys. Chem. Chem. Phys.* **2019**, *21*, 11578.

[23] Parashchuk, O. D.; Mannanov, A. A.; Konstantinov, V. G.; Dominskiy, D. I.; Surin, N. M.; Borshchev, O. V.; Ponomarenko, S. A.; Pshenichnikov, M. S.; Paraschuk, D. Y. *Adv. Funct. Mater.* **2018**, *28*, 1800116.

[24] Skorotetcky, M. S.; Borshchev, O. V.; Surin, N. M.; Meshkov, I. B.; Muzafarov, A. M.; Ponomarenko, S. A. *Silicon* **2015**, *7*, 191.

[25] Zhang, Y.; Xie, S.; Zeng, Z.; Tang, B. Z. *Matter* **2020**, *3*, 1862.

[26] Wang, L.; Wang, L.; Yang, X.; Li, W.; Chen, L.; Tang, J.; Cong, W.; Hu, R.; Tebyetekerwa, M.; Tang, B. *Prog. Org. Coat.* **2022**, *163*, 106633.

[27] Li, W.; Ding, Y.; Tebyetekerwa, M.; Xie, Y.; Wang, L.; Li, H.; Hu, R.; Wang, Z.; Qin, A.; Tang, B. Z. *Mater. Chem. Front.* **2019**, *3*, 2491.

[28] Li, J.; Shan, T.; Yao, M.; Gao, Y.; Han, X.; Yang, B.; Lu, P. *J. Mater. Chem. C* **2017**, *5*, 2552.

[29] Gong, W.-L.; Wang, B.; Aldred, M. P.; Li, C.; Zhang, G.-F.; Chen, T.; Wang, L.; Zhu, M.-Q. *J. Mater. Chem. C* **2014**, *2*, 7001.

[30] Zheng, X.; Zhu, W.; Zhang, C.; Zhang, Y.; Zhong, C.; Li, H.; Xie, G.; Wang, X.; Yang, C. *J. Am. Chem. Soc.* **2019**, *141*, 4704.

[31] Mu, C.; Zhang, Z.; Hou, Y.; Liu, H.; Ma, L.; Li, X.; Ling, S.; He, G.; Zhang, M. *Angew. Chem., Int. Ed.* **2021**, *60*, 12293.

[32] Ni, Y.; Zhang, S.; He, X.; Huang, J.; Kong, L.; Yang, J.; Yang, J. *Anal. Methods* **2021**, *13*, 2830.

[33] Feng, H.; Zhou, Z.; May, A. K.; Chen, J.; Mack, J.; Nyokong, T.; Gai, L.; Lu, H. *J. Mater. Chem. C* **2021**, *9*, 6470.

[34] Xiang, X.; Zhou, Z.; Feng, H.; Feng, S.; Gai, L.; Lu, H.; Guo, Z. *CCS Chem.* **2020**, *2*, 329.

[35] Feng, S.; Zhou, Z.; Xiang, X.; Feng, H.; Qu, Z.; Lu, H. *ACS Omega*

2020, *5*, 19181.
[36] Zheng, X.; Du, W.; Gai, L.; Xiao, X.; Li, Z.; Xu, L.; Tian, Y.; Kira, M.; Lu, H. *Chem. Commun.* **2018**, *54*, 8834.
[37] Wang, S.; Lu, H.; Wu, Y.; Xiao, X.; Li, Z.; Kira, M.; Shen, Z. *Chem.-Asian J.* **2017**, *12*, 561.
[38] Yamanoi, Y.; Nishihara, H. *J. Org. Chem.* **2008**, *73*, 6671.
[39] Bunker, C. E.; Hamilton, N. B.; Sun, Y. P. *Anal. Chem.* **1993**, *65*, 3460.
[40] Shih, P.-I.; Chuang, C.-Y.; Chien, C.-H.; Diau, E. W.-G.; Shu, C.-F. *Adv. Funct. Mater.* **2007**, *17*, 3141.
[41] Beiting, E. J.; Zeringue, K. J.; Stickel, R. E. *Spectrochim. Acta* **1985**, *41*, 1413.
[42] Shimada, M.; Tsuchiya, M.; Sakamoto, R.; Yamanoi, Y.; Nishibori, E.; Sugimoto, K.; Nishihara, H. *Angew. Chem.*, *Int. Ed.* **2016**, *55*, 3022.
[43] Tao, T.; Gan, Y.; Zhao, Y.; Yu, J.; Huang, Q.; Yang, Z.; Chen, M.; Huang, W. *J. Mater. Chem. C* **2019**, *7*, 3765.

(Zhao, C.)

